A Simple Signal Processing Architecture for Instantaneous Radar Polarimetry

Stephen D. Howard, A. Robert Calderbank, *Fellow, IEEE*, and William Moran, *Member, IEEE*

***Abstract*—This paper describes a new radar primitive that enables instantaneous radar polarimetry at essentially no increase in signal processing complexity. This primitive coordinates transmission of distinct waveforms on orthogonal polarizations and applies a unitary matched filter bank on receive. This avoids the information loss inherent in single-channel matched filters. A further advantage of this scheme is the elimination of range sidelobes.**

***Index Terms*—Golay complementary waveforms, multiple-input multiple-output (MIMO) radar, radar detection, radar polarimetry, radar signal processing, radar waveforms, unitary matched filters.**

I. Introduction

POLARIMETRIC radar techniques are employed in remote sensing and synthetic aperture radar (see [1]–[4]). Their success in discriminating diverse regions in radar images demonstrates the value of using all dimensions of the polarization scattering matrix and motivates the use of polarimetry for target detection in a dynamic clutter environment. This requires a new radar primitive that makes the polarization scattering matrix available on a pulse-by-pulse basis at a computational cost comparable to single-channel matched filtering. Our approach takes advantage of recent advances in radar hardware technology that make it possible for radar systems to transmit different waveforms on multiple spatial and/or polarization channels simultaneously. This functionality represents an enormous opportunity for waveform design as demonstrated by the literature on this topic [5]–[10]. The introduction of multiple antennas increases the degrees of freedom in the waveform design space.

There are many proposals for multichannel radar, emanating from the conventional *monostatic* radar system where transmitter and receiver are collocated. Collocation makes it easy for transmitter and receiver to share a common stable clock (local oscillator), which is required for both range and Doppler measurements. Signal processing for multistatic radars (see [11]) with widely dispersed antenna elements is currently a very active research area, in part because of significant advances in hardware capabilities. Multistatic radar enables multiple views of the scene, and a (wide-angle) tomographic approach to the recovery of the scene from the data. A major advantage of multistatic radar is substantial improvement in detection due to multiple views of the target being available. When system elements are widely dispersed, the coherent implementation of multistatic radar is rendered difficult by the problem of clock synchronization, though Global Positioning System (GPS) and network technologies have rendered these problems more tractable. An additional challenge is the degree of computation necessary to recover the scene, or detect a target, by integrating multiple views.

It is natural to approach multichannel radar in terms of spatial diversity concepts developed for multiple-input multiple-output (MIMO) communications ([5], [12]). Performance improvements in MIMO communications derive from spatial diversity, that is, the statistical independence of the different channels provided by the multiple antenna elements. Fishler *et al.* [12] correctly point out that sufficiently separated system elements do give rise to statistically independent views of the target. However, in their analysis of detection performance, they assume a target in the far field by invoking a "narrowband" approximation which necessarily implies complete statistical dependence across the distributed antennas. Without the narrowband approximation, the analysis reduces to that of conventional multistatic radar systems.

In this paper, we focus on polarization diversity, and we propose an approach to MIMO radar that uses polarization to provide essentially independent channels for viewing target and clutter. The four dimensions of the scattering matrix enable discrimination of target from clutter by making structure evident that is not apparent in any one-dimensional projection. Target scattering profiles depend significantly both on aspect angle and illumination and receive polarizations (see Skolnik [13, Sec. 2.7]). Polarization diversity enables detection of smaller radar cross section (RCS) targets, and avoids the physical, mathematical, and engineering challenges of time-of-arrival coherent combining. The advantage of polarization diversity over spatial diversity is that diversity gains are possible with collocated antennas.

We develop an analogue of the Alamouti space–time block code [14] that coordinates transmission of waveforms over two orthogonal polarizations. The components are Golay pairs [15]

Manuscript received January 14, 2006; revised November 23, 2006. This work was supported in part by the Defense Advanced Research Projects Agency of the U.S. Department of Defense and was monitored in part by the Air Force Office of Scientific Research, under Contracts HR0011-0501-0030 and FA9550-04-1-0431. This project is proudly supported by International Science Linkages established under the Australian Government's innovation statement, "Backing Australia's Ability." The United States Government is authorized to reproduce and distribute reprints for governmental purposes notwithstanding any copyright notation hereon.

S. D. Howard is with the Defence Science and Technology Organization, P.O. Box 1500, Edinburgh, 5111, Australia.

A. R. Calderbank is with the Program in Applied and Computational Mathematics, Princeton University, Princeton, NJ 08544 USA.

W. Moran is with the Department of Electrical and Electronic Engineering, The University of Melbourne, Vic. 3010, Australia.

Communicated by A. Høst-Madsen, Associate Editor for Detection and Estimation.

Digital Object Identifier 10.1109/TIT.2007.892809

of phase-coded waveforms and the quadrature mirror property of Golay complementary sequences defines a unitary matched filter that provides access to the full polarization scattering matrix on a pulse-by-pulse basis. Golay complementary sequences are used to eliminate range sidelobes in single-channel radar, and this important property is preserved here. Hence this triple play of polarization, Golay technology, and Alamouti codes has the potential to significantly improve the performance of any conventional polarimetric radar.

II. Instantaneous Radar Polarimetry

Space–time codes, introduced by Tarokh *et al.* [16] improve the reliability of communication over fading channels by correlating signals across different transmit antennas. The Alamouti code (see [14]) is described by a 2×2 matrix, where the columns represent different time slots, the rows represent different antennas, and the entries are the symbols to be transmitted. The reason for intense commercial interest in this code is that both coherent and noncoherent detection are remarkably simple. It is possible to separate the data streams transmitted from the two antennas using only linear processing at the receiver. This means that the end-to-end complexity of signal processing is essentially the same as for single-antenna systems.

The encoding rule is

$$(c_1, c_2) \rightarrow \begin{pmatrix} c_1 & c_2 \\ -\bar{c}_2 & \bar{c}_1 \end{pmatrix}. \qquad (1)$$

The signals r_1, r_2 received over two consecutive time slots are given by

$$\begin{pmatrix} r_1 & r_2 \end{pmatrix} = \begin{pmatrix} g_1 & g_2 \end{pmatrix} \begin{pmatrix} c_1 & c_2 \\ -\bar{c}_2 & \bar{c}_1 \end{pmatrix} + \begin{pmatrix} z_1 \\ z_2 \end{pmatrix} \qquad (2)$$

where g_1, g_2 are the path gains from the two transmit antennas to the mobile, and the noise samples z_1, z_2 are independent samples of a zero-mean complex Gaussian random variable with noise energy N_0 per complex dimension. Thus

$$\boldsymbol{r} = \boldsymbol{g}\boldsymbol{C} + \boldsymbol{z} \qquad (3)$$

where the matrix $\boldsymbol{C}$ is orthogonal. Channel estimation in communications is the analogue of radar image formation. The path gains $\boldsymbol{g}$ between the base station and the mobile are estimated by choosing c_1 and c_2 to be known pilot tones. The receiver then forms

$$\boldsymbol{r}\boldsymbol{C}^* = (|c_1|^2 + |c_2|^2)\boldsymbol{g} + \boldsymbol{z}_0 \qquad (4)$$

where $\boldsymbol{z}_0$ is still white, so that g_1, g_2 can be estimated separately rather than jointly, which is more complex. Space–time codes have been shown to be robust against nonideal operating conditions such as antenna correlation, channel estimation errors, and Doppler effects [16], [17]. We also note that field tests have been conducted in real mobile wireless environments to explore the benefits of increased diversity order using spatially separated polarized antennas at the base station receiver of a code-division multiple-access (CDMA) cellular system [18].

Current polarimetric radar systems are capable of serial transmission using two orthogonal polarizations. Typically, the radar separates the two orthogonal polarizations by transmitting a waveform on one polarization followed by a second waveform on the orthogonal polarization. The radar receives on both polarizations simultaneously but is not able to form an *instantaneous* measurement of the full scattering matrix. However, there is no technology roadblock to deployment of a radar that is capable of transmitting and receiving in two orthogonal polarizations simultaneously. In fact, the Naval Research Laboratory maintains an experimental radar platform that is able to support this functionality [19]. The combined signal then has an electric field vector that is modulated both in direction and amplitude by the waveforms on the two polarization channels, and the receiver is used to obtain both components of the reflected waveform. The polarization diversity technique proposed in this paper improves performance of such an enhanced polarimetric radar.

The radar cross section of an extended target such as an aircraft or a ship is highly sensitive to the angle of incidence and angle of view of the sensor (see [13, Secs 2.7–2.8]). In general, the reflection properties that apply to each polarization component are also different, and indeed reflection can change the direction of polarization. Thus, polarimetric radars are able to obtain the scattering tensor of a target

$$\boldsymbol{\Sigma} = \begin{pmatrix} \sigma_{VV} & \sigma_{VH} \\ \sigma_{HV} & \sigma_{HH} \end{pmatrix} \qquad (5)$$

where σ_{VH} denotes the target scattering coefficient into the vertical polarization channel due to a horizontally polarized incident field. The polarization diversity technique proposed in this paper provides concurrent rather than serial access to the cross-polarization components of the scattering tensor, which varies more rapidly in standard radar models used in target detection and tracking [20], [21] than in models used in remote sensing or synthetic aperture radar.

In fact, what is measured is the combination of three matrices

$$\boldsymbol{H} = \begin{pmatrix} h_{VV} & h_{VH} \\ h_{HV} & h_{HH} \end{pmatrix} = \boldsymbol{C}_{\mathrm{Rx}}\boldsymbol{\Sigma}\boldsymbol{C}_{\mathrm{Tx}}, \qquad (6)$$

where C_{Rx} and C_{Tx} correspond to the polarization coupling properties of the transmit and receive antennas, whereas $\boldsymbol{\Sigma}$ results from the target. In most radar systems, the transmit and receive antennas are common, and so the matrices C_{Tx} and C_{Rx} are conjugate. The cross-coupling terms in the antenna polarization matrices are clearly frequency and antenna-geometry dependent but for the linearly polarized case this value is typically no better than about -20 dB.

We propose to use both polarization modes to transmit four quaternary phase-shift keying (QPSK) waveforms $w_H^1, w_V^1, w_H^2, w_V^2$. On each polarization mode, we transmit two QPSK-coded pulses separated by a time interval T or pulse repetition interval (PRI). Thus, we transmit a first pair of waveforms $\boldsymbol{w}^1 = (w_V^{(1)}, w_H^{(1)})$ followed by a second pair of waveforms $\boldsymbol{w}^2 = (w_V^{(2)}, w_H^{(2)})$.

This *vector-valued* waveform passes through the channel defined by the target and antennas to give vectors $\boldsymbol{r}^j$ at the receiver, so that for each time slot j

$$\boldsymbol{r}^j = \begin{pmatrix} r_V^j \\ r_H^j \end{pmatrix} = \boldsymbol{H}\boldsymbol{w}^j + \boldsymbol{z}^j \qquad (7)$$

where the $\boldsymbol{z}^j$ are white Gaussian noise.

We now develop an analogue of the Alamouti space–time block code to coordinate transmission over the V and H channels, where the entries are QPSK-valued sequences rather than complex numbers, and multiplication is replaced by convolution. Define

$$w_H^2 = \widetilde{w_V^1} \tag{8}$$

$$w_V^2 = -\widetilde{w_H^1} \tag{9}$$

where $\tilde{\cdot}$ denotes complex conjugate time reversal.

The phase-coded waveforms $w_V^1(D)$ and $w_H^1(D)$ are viewed as polynomials in the delay operator D, and their coefficients are fourth roots of unity since these are QPSK waveforms. For example, we may represent the QPSK-coded sequence $w = (1, 1, 1, -1, 1, 1, -1, 1)$ as the polynomial $w(D)$ given by

$$w(D) = D^7 + D^6 + D^5 - D^4 + D^3 + D^2 - D + 1. \tag{10}$$

The complex conjugate time reverse of $w(D)$ is

$$\tilde{w}(D) = D^7 - D^6 + D^5 + D^4 - D^3 + D^2 + D + 1. \tag{11}$$

In general, given a polynomial $w(D)$, the complex conjugate time-reversed polynomial $\tilde{w}(D)$ is given by

$$\tilde{w}(D) = D^{\deg w}\overline{w}(D^{-1}) \tag{12}$$

where $\deg w$ is the degree w, and $^{-}$ denotes complex conjugation.

Regarding the returns $r_V^j(D)$ and $r_H^j(D)$ also as polynomials in the delay operator, we combine the two equations comprising (7) into

$$\boldsymbol{R} = (\boldsymbol{r}^1(D), \boldsymbol{r}^2(D)) = \boldsymbol{HW} + \boldsymbol{Z} \tag{13}$$

where

$$\boldsymbol{W} = \begin{pmatrix} w_V^1(D) & -\widetilde{w_H^1}(D) \\ w_H^1(D) & \widetilde{w_V^1}(D) \end{pmatrix} \tag{14}$$

and

$$\boldsymbol{H} = \begin{pmatrix} h_{VV} & h_{VH} \\ h_{HV} & h_{HH} \end{pmatrix}.$$

The entries of $\boldsymbol{H}$ are taken to be constant since they correspond to a fixed range and a fixed time. We note that, in reality, $\boldsymbol{H}$ is a function of range, and in this model is also a function of the delay operator. However, since all operations performed in our scheme are (time-invariant) filters, it will be enough for our purposes to work with this fixed snapshot. Moreover, the intrusion of the delay operator suggests, somewhat misleadingly, a discretization of the scene at the chip rate (of the delay operator). In fact, it is not hard to see that the ensuing analysis works in continuous time with the "Dirac delta" being replaced by a triangle function of double the chip length.

We now show that if we require the matrix $\boldsymbol{W}$ to be unitary, then it is easy to estimate the scattering matrix $\boldsymbol{H}$. The unitary condition is equivalent to

$$w_V^1(D)\widetilde{w_V^1}(D) + w_H^1(D)\widetilde{w_H^1}(D) = 2\left(\deg w_V^1 + 1\right) D^{\deg w_V^1}. \tag{16}$$

Polynomials with coefficients that are fourth roots of unity and that satisfy (16) are complex Golay complementary pairs [22]. These include the classical Golay pairs whose coefficients are ± 1. Golay pairs are widely studied in the radar and communications literature both as pairs and individually. As individual waveforms they have good autocorrelation properties. These pairs have been constructed, in particular, with lengths 2^n for all positive integers n [23]. They have excellent peak-to-average spectral properties [24].

The unitary condition means that it is possible to separate the four channels HH, HV, VH, VV at the receiver using only linear processing. The four matched filters are given by

$$\boldsymbol{Q} = \begin{pmatrix} m_1 * r_V & m_2 * r_V \\ m_1 * r_H & m_2 * r_H \end{pmatrix} \tag{17}$$

where

$$m_1(D) = \widetilde{w_V^1}(D)D^N - w_H^1(D)$$
$$m_2(D) = \widetilde{w_H^1}(D)D^N + w_V^1(D). \tag{18}$$

The analogue of (4) is

$$\boldsymbol{R}\tilde{\boldsymbol{W}} = \boldsymbol{HW}\tilde{\boldsymbol{W}} + \boldsymbol{Z}' \tag{19}$$

which combined with (14) gives

$$\boldsymbol{R}\tilde{\boldsymbol{W}} = \left(w_V^1(D)\widetilde{w_V^1}(D) + w_H^1(D)\widetilde{w_H^1}(D)\right)\boldsymbol{H} + \boldsymbol{Z}'. \tag{20}$$

Now (16) gives

$$\boldsymbol{R}\tilde{\boldsymbol{W}} = 2(\deg w_V^1 + 1)D^{\deg w_V^1}\boldsymbol{H} + \boldsymbol{Z}' \tag{21}$$

so that the four scattering coefficients can be recovered with delay $\deg(w)$.

Remark 1: Radar signal processing is complicated by sidelobes arising from the convolution of the scene with the autocorrelation of the illuminating waveforms. Extensive work has been done on waveform design for the manipulation of waveform sidelobes (see Levanon [25]). In particular, previous work on single-channel radar employs consecutive transmission of Golay complementary waveforms to eliminate range sidelobes and produce a "thumbtack" autocorrelation [26]. Note that cross correlation between waveforms separated by one or more PRIs produces range aliasing which is attenuated by distance, and may be mitigated by varying the PRIs.

Four-channel signal processing as described above combines instantaneous access to the full polarization scattering matrix with the elimination of range sidelobes. In addition, range-aliasing sidelobes are smaller than in single-channel radars using sequences of identical pulses, because the four waveforms comprising the matrix $\boldsymbol{W}$ are mutually orthogonal [27].

Remark 2: Matched filtering at the front end of radar signal processing in one dimension (for example, single polarization) always incurs a loss of information, since the received signal cannot be recovered from the matched filter output. However, four-channel signal processing as described above incurs no loss of information since the matched filter bank is unitary.

Remark 3: The description above suggests that a radar image will be available only on every second pulse, since two PRIs are required to form an image. In fact, after the transmission of the first pulse, images can be available at every PRI. This is done by reversing the roles of the waveforms transmitted on the two pulses. Thus, in the analysis, the matrix $\boldsymbol{W}$ in (14) is replaced by

$$\boldsymbol{V} = \begin{pmatrix} -\widetilde{w_H^1}(D) & w_V^1(D) \\ \widetilde{w_V^1}(D) & w_H^1(D) \end{pmatrix} \tag{22}$$

which, because of (16), is still unitary. Moreover, the processing involved is essentially invariant from pulse to pulse: the return pulse in each of the H and V channels is correlated against the transmit pulse on that channel. This yields an estimate of the scattering matrix on each pulse.

Remark 4: An alternative approach to single-channel radar signal processing is to solve an inverse problem in order to avoid the loss incurred by matched filtering. This method is notoriously sensitive to receiver noise. In four-channel signal processing, as described above, inversion and matched filtering coincide, since the filter bank is unitary, and instabilities do not occur.

Remark 5: It would appear from (16) that the correlation sidelobes vanish only at delays that are multiples of the chip length, but in fact it is a property of Golay pairs that it actually holds for all possible nonzero delays. It is this property that enables detection based on energy thresholds that is independent of polarization cross coupling of the antenna. Signal processing complexity is essentially the same as for the baseline radar system; all that changes is the initial matched filter.

Remark 6: Diversity requires waveforms transmitted from different antennas be reflected in different ways from the target. This is true for differently polarized waveforms and for waveforms that are transmitted from sufficiently spatially separated antennas. The advantage of polarization diversity is that time synchronization of the vertical and horizontal returns from a target is automatic, so that we avoid the complication of time-of-arrival signal processing.

Remark 7: Our aim of obtaining instantaneous radar polarimetry is shared with a technique described in [28]. Its authors propose the use of waveforms with uniformly low cross correlations in the two polarization channels. In this way, they achieve approximate separation on each pulse and are thereby able to obtain the full scattering matrix. They give several instances of such waveforms including linear frequency-modulated waveforms, frequency-separated waveforms, and phase-coded waveforms. There are several issues with each of these techniques, but perhaps the most important from the perspective of this paper are that they are unable to provide the unitarity and zero-sidelobe performance of the ones proposed in this paper.

Remark 8: As we indicated in Remark 7, the paper of Giuli *et al.* [28] suggests frequency separation as a means of providing the channel separation that we achieve by using consecutive pulses. A major problem with the use of frequency separation in this way is that the phase of a return from a scatterer depends on the range of that scatterer measured in carrier wavelengths. A change of frequency changes that phase. As a result, the frequency separation method described in [28] would give a scattering matrix for a given scatterer would vary with range. We intend to address the problem of frequency separation of waveforms in a future publication.

Remark 9: An alternative scheme for measuring the scattering matrix, involving switching the transmit polarization on a pulse-by-pulse basis, is currently in use. This has the advantage of requiring only one transmit channel, but fails to provide either unitary processing or zero sidelobes. We remark that, while presented in terms of dual channel transmission, our method can be implemented in a single-channel system capable of switching polarization at the chip rate.

III. Detection in Noise

It is natural to approach multichannel radar in terms of spatial diversity concepts developed for MIMO communications. Diversity gains are typically expressed in terms of energy required for detection in noise. This criterion applies directly to particular radar scenarios in which detection is noise limited and early detection of a slowly fluctuating target is the goal. Detection in clutter is discussed in the next section. We now evaluate the detection in noise aspects of instantaneous radar polarimetry following the classic treatment of van Trees [20].

We assume a slowly fluctuating point target model (Swerling 1, see [21]); that is, we take the matrix $\boldsymbol{H}$ (considered as a four-component vector $\boldsymbol{h}$) as zero mean Gaussian distributed with covariance matrix $\boldsymbol{\Lambda}$. In this section, to provide insight while retaining simplicity of analysis, we will also make the assumption that the components of $\boldsymbol{H}$ are independent and identically distributed, so that $\boldsymbol{\Lambda} = 2\sigma^2\boldsymbol{I}$. We will also assume that the noise in each channel of the receiver is additive zero-mean Gaussian white noise with power N_0. At the end of this section, we include a simulation study where the gains predicted by this simple model are realized by a full-scale electromagnetic (EM) simulation of a large complex target. The detection statistic is then $\|\boldsymbol{Q}\|_2^2$, where

$$\boldsymbol{Q} = \begin{pmatrix} m_1 * r_V & m_2 * r_V \\ m_1 * r_H & m_2 * r_H, \end{pmatrix} \tag{23}$$

and $\|\cdot\|_2$ represents the Frobenius norm. Here r_V and r_H are the complete returns for the two polarization channels; that is, they are not considered to be separated into two time slots.

We now provide a single pulse detection analysis and the baseline for comparison is target detection for a single channel. Note that typical radar signal processing increases probability of detection through coherent or incoherent integration over multiple pulses. These methods apply equally well to four-channel signal processing.

We assume the pulses w_V and w_H have unit energy and that the total transmit energy across the two polarization channels is E_t. The detection problem then becomes

$$\boldsymbol{q} = \begin{cases} 2\sqrt{E_t/4}\,\boldsymbol{h} + \boldsymbol{n} & : H_1 \\ \boldsymbol{n} & : H_0 \end{cases} \tag{24}$$

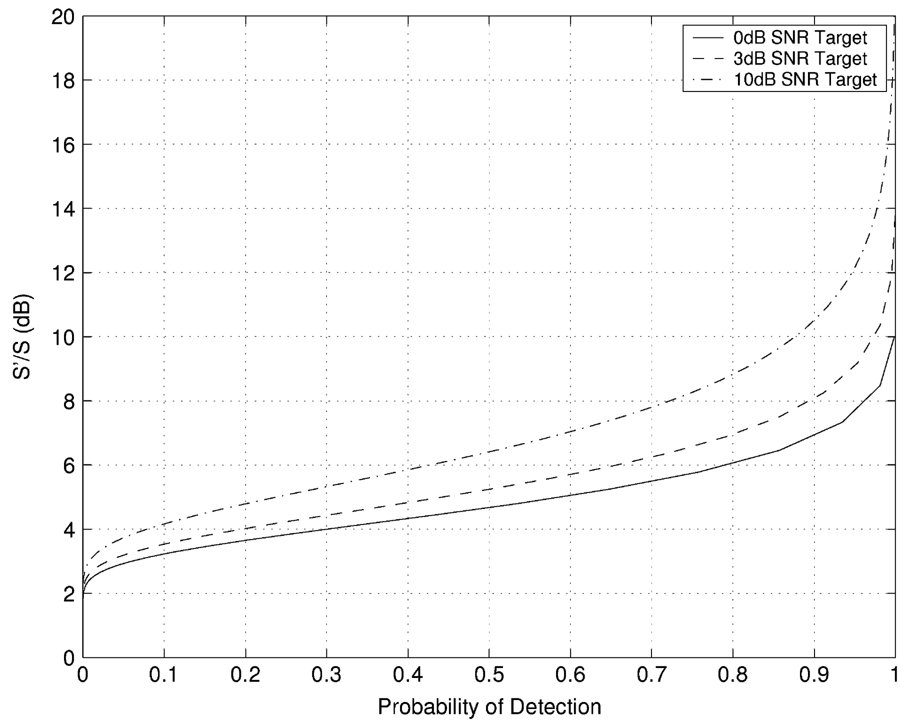

Fig. 1. The fraction of extra SNR at the receiver (S'/S) which is needed by a single-channel system to give the same probability of detection and probability of false alarm as our new scheme.

where H_1 denotes the hypothesis that the target is present and $\boldsymbol{q}$ is the four-component vector corresponding to $\boldsymbol{Q}$. The properties of the waveforms w_V and w_H imply that $E(\boldsymbol{n}\boldsymbol{n}^\dagger) = 2N_0\boldsymbol{I}$. As we have mentioned under the assumption that the target covariance matrix is $\boldsymbol{\Lambda} = 2\sigma^2\boldsymbol{I}$; that is, the four components of the target scattering matrix have equal variance, the likelihood ratio detector is equivalent to the test

$$||\boldsymbol{q}||^2 > \gamma \tag{25}$$

for some threshold $\gamma > 0$. The probability of false alarm for this detector is

$$\begin{aligned} P_F &= \Pr(||\boldsymbol{q}||^2 > \gamma | H_0) \\ &= \frac{1}{48N_0^4}\int_{\sqrt{\gamma}}^{\infty} z^7 \exp(-z^2/2N_0)\, dz \\ &= \Phi\left(\frac{\gamma}{2N_0}\right) \end{aligned} \tag{26}$$

where

$$\Phi(x) = \left(1 + x^2 + \frac{1}{2}x^3 + \frac{1}{6}x^3\right) e^{-x}. \tag{27}$$

Similarly, the probability of detection is

$$\begin{aligned} P_D &= \Pr(||\boldsymbol{q}||^2 > \gamma | H_1) \\ &= \Phi\left(\frac{\gamma}{2\sigma^2 E_t + 2N_0}\right). \end{aligned} \tag{28}$$

We compare (28) to the result for a conventional single-channel radar in which a waveform of energy E_t (the same total energy as for our polarization scheme) is transmitted. To be specific, we might take the waveform transmitted on the single-channel system to be the waveform transmitted on the V channel of the dually polarized system. We observe that the waveforms transmitted in the four-channel system each have the same time–bandwidth product (equal to that of the waveform transmitted in the single-channel system).

The receiver operating characteristic (ROC) curve for the single-channel radar, under the above target assumptions, is of the form (van Trees, [20, Ch. 9])

$$P_F = P_D^{(S+1)} \tag{29}$$

where $S = \sigma^2 E_t/N_0$ is the signal-to-noise ratio (SNR) at the receiver.

In order to compare our new scheme with a conventional single polarization channel radar we consider the increased SNR S' that the conventional radar needs to ensure the same P_D for a given P_F as our new scheme. Using (29) with P_F and P_D given by (26) and (28) respectively, we have

$$\frac{S'}{S} = \frac{\log\left(\Phi\left(\frac{\gamma}{2N_0}\right)/\Phi\left(\frac{\gamma}{N_0(S+1)}\right)\right)}{S\log\Phi\left(\frac{\gamma}{N_0(S+1)}\right)}. \tag{30}$$

This ratio of SNRs is shown in Fig. 1 for targets with various SNRs S at the receiver. We notice that, for any reasonable value of probability of detection (e.g., $P_D > 0.5$), our technique gives equivalent performance to a single-channel radar for substantially smaller transmit energy or alternatively, allows detection at substantially greater ranges for a given transmit energy.

Finally, we note that it is possible under some circumstances that the cross sections for the HV and VH channels may be substantially smaller in magnitude than the VV and HH channels. To show that our scheme still provides significant improvement

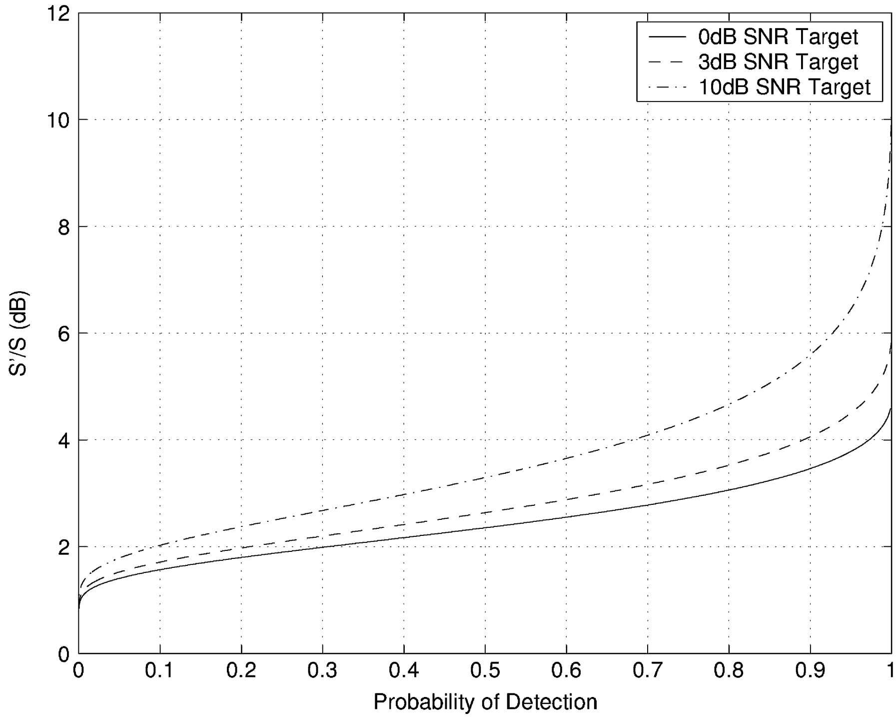

Fig. 2. The fraction of extra SNR at the receiver (S'/S) which is needed by a single-channel system to give the same probability of detection and probability of false alarm as our new scheme using only the VV and HH channels.

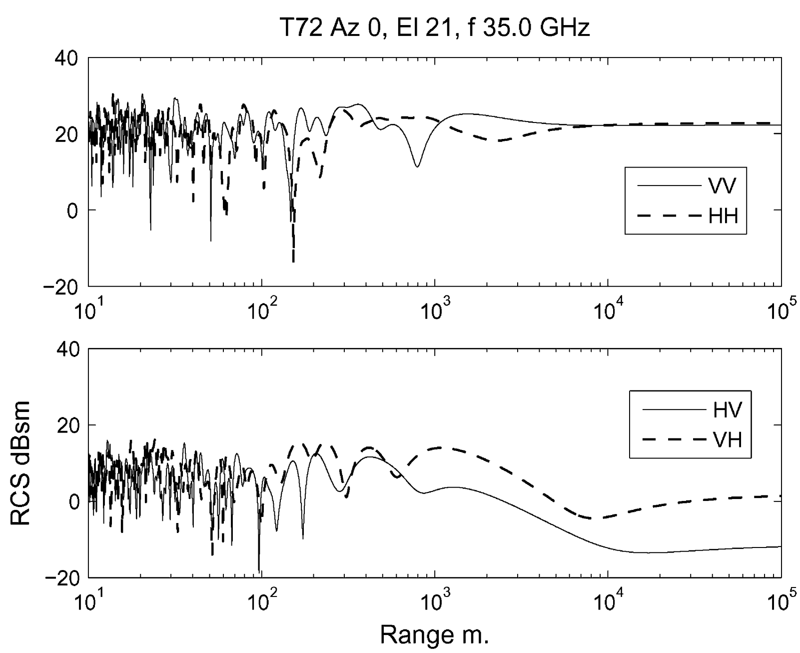

Fig. 3. Simulation of polarization returns from a large complex target.

in this case, we assume that h_{HV} and h_{VH} are zero and follow through the above analysis using only channels 1 and 3 in (23). There is again a relation between S' and S of the form (30), but with $\Phi(x)$ replaced by the function $\Phi_2(x) = (1+x)e^{-x}$. This ratio of SNRs for this case is shown in Fig. 2 for targets generating various SNRs S at the receiver of our radar. We see that even in this case our scheme still provides a substantial improvement, but not as great as that shown in Fig. 1 for the full scheme, where the elements of the $\boldsymbol{H}$ matrix have equal variances. In general, the improvement in detection probability made possible by our scheme will be somewhere between these two extremes.

Remark 10: We are able to improve detection performance by using longer pulse trains. The waveform matrix is no longer square and the appropriate generalization of the Alamouti matrix is a rectangular orthogonal design [29]. The inverse of $\boldsymbol{W}$ is now replaced by $\boldsymbol{W}'$ such that $\boldsymbol{W}'\boldsymbol{W} = \lambda I$ for some scalar λ where $|\lambda| > 1$.

High-fidelity EM simulation provides insight into the polarization returns from large complex targets. Fig. 3 is provided by Raytheon Missile Systems [30] and measures radar cross section in decibels per square meter as a function of range for a large complex target (Swerling 1 and 3 target models) with about 500 highly correlated scattering centers. In this study the VH and HV components are more than 8 dB below the VV and HH components.

The Raytheon simulation study of four-channel signal processing predicts gains after pulse integration of about 5 dB at representative target SNRs, which is consistent with the detection analysis provided in this paper for simple Gaussian models of a single-point scatterer. Details will appear elsewhere.

IV. Discrimination in Clutter

The dramatic success of polarimetric radar techniques in remote sensing and synthetic aperture radar demonstrates the advantages of using all of the dimensions of the polarization scattering matrix to discriminate diverse regions in radar images ([1]–[4]). The four scattering dimensions make structure evident that is not readily apparent in any one-dimensional projection. However, there is a loss of information incurred by taking longer term averages, and one value of instantaneous radar polarimetry is to change the time scale on which the statistics can be exploited. Since there are no range sidelobes, it also provides a more focused measurement of the data.

The availability of short time-scale clutter measurements has been shown to dramatically improve detection probability [31] in dynamic clutter. We expect significant further improvements from instantaneous radar polarimetry.

V. Conclusion

We have described a signal processing architecture that enables instantaneous radar polarimetry at essentially no increase in signal processing complexity over conventional single-channel matched filtering. This signal processing architecture avoids the loss of information inherent in matched filtering at the front end of single-channel radar processing. This is possible because the mached filter bank is unitary. The signal processing architecture provides instantaneous access to the full polarization scattering matrix with the elimination of range sidelobes.

We have explored applicability to particular radar scenarios in which detections are noise limited and early detection of a slowly fluctuating target is the goal. We have compared our scheme to a conventional single polarization channel radar and have shown that for an idealized point target model and for reasonable values of the probability of detection in noise it gives equivalent performance to the baseline system for substantially smaller transmit energy. The predicted gains are consistent with the results of an EM simulation of a large complex target.

In future work, we expect to report on experimental data from the Naval Research Laboratory [19]. Future theoretical work will focus on the integration of this new radar primitive within a complete radar signal processing receiver architecture.

Acknowledgment

The authors are grateful to A. Samuel, M. Frank, and H. A. Schmitt of Raytheon Missile Systems for performing the polarization diversity simulation study.

References

[1] C. López-Martínez, E. Pottier, and S. R. Cloude, "Statistical assessment of eigenvector-based target decomposition theorems in radar polarimetry," *IEEE Trans. Geosci. Remote Sens.*, vol. 43, no. 9, pp. 2058–2073, Sep. 2005.

[2] A. Reigber, K. Papathanassiou, S. Cloude, and A. Moreira, "SAR tomography and interferometry for the remote sensing of forested terrain," *Zeitschrift für Telekommunikation (J. Telecommun.), EUSAR 2000 Special Issue, Frequenz*, , vol. 55, pp. 119–122, 2001.

[3] J.-S. Lee, M. Grunes, T. Ainsworth, L.-J. Du, D. Schuler, and S. Cloude, "Unsupervised classification using polarimetric decomposition and the complex Wishart classifier," *IEEE Trans Geosci. Remote Sens.*, vol. 37, no. 5, pp. 2249–2258, Sep. 1999.

[4] Y.-Q. Jin and S. Cloude, "Numerical eigenanalysis of the coherency matrix for a layer of random nonspherical scatterers," *IEEE Trans. Geosci. Remote Sens.*, vol. 32, no. 6, pp. 1179–1185, Nov. 1994.

[5] E. Fishler, A. Haimovich, R. Blum, R. Cimini, D. Chizhik, and R. Valenzuela, "Performance of MIMO radar systems: Advantages of angular diversity," in *Conf. Rec. 38th Asilomar Conf. Signals, Systems and Computers*, Pacific Grove, CA, Nov. 2004, vol. 1, pp. 3–5–309.

[6] K. Forsythe, D. Bliss, and G. Fawcett, "Multiple-input multiple-output (MIMO) radar: Performance issues," in *Confe. Rec. 38th Asilomar Conf. Signals, Systems and Computers*, Pacific Grove, CA, Nov. 2004, vol. 1, pp. 310–315.

[7] F. Robey, S. Coutts, D. Weikle, J. McHarg, and K. Cuomo, "MIMO radar theory and experimental results," in *Conf. Rec. 38th Asilomar Confe. Signals, Systems and Computers*, Pacific Grove, CA, Nov. 2004, vol. 1, pp. 300–304.

[8] G. San Antonio and D. R. Fuhrmann, "Beampattern synthesis for wideband MIMO radar systems," in *Proc. 1st IEEE Int. Workshop on Computational Advances in Multi-Sensor Adaptive Processing*, Puerto Vallarta, Mexico, Dec. 2005, pp. 105–108.

[9] D. R. Fuhrmann and G. San Antonio, "Transmit beamforming for MIMO radar systems using partial signal correlation," in *Conf. Rec. 38th Asilomar Conf. Signals, Systems and Computers*, Pacific Grove, CA, Nov. 2004, vol. 1, pp. 295–299.

[10] L. White and P. Ray, "Signal design for MIMO diversity systems," in *Conf. Rec. 38th Asilomar Conf. Signals, Systems and Computers*, Pacific Grove, CA, Nov. 2004, pp. 973–977.

[11] F. Gini, A. Farina, and M. Greco, "Selected list of references on radar signal processing," *IEEE Trans. Aerosp. Electron. Syst.* , vol. 37, no. 1, pp. 329–359, Jan. 2001.

[12] E. Fishler, A. Haimovich, R. Blum, D. Chizhik, L. Cimini, and R. Valenzuela, "MIMO radar: An idea whose time has come," in *Proc. IEEE Radar Conf.*, New York, 2004, pp. 71–78.

[13] M. I. Skolnik, *Introduction to Radar Systems*, 3rd ed. New York: McGraw-Hill, 2001.

[14] S. Alamouti, "A simple transmit diversity technique for wireless communications," *IEEE J. Select. Areas Commun.*, vol. 16, no. 8, pp. 1451–1458, Oct. 1998.

[15] M. J. E. Golay, "Static multislit spectrometry and its application to the panoramic display of infrared spectra," *J. Opt. Soc. Amer.*, vol. 41, pp. 468–472, 1951.

[16] V. Tarokh, A. Naguib, N. Seshadri, and A. Calderbank, "Space–time codes for high data rate wireless communication: Performance criteria in the presence of channel estimation errors, mobility, and multiple paths.," *IEEE Trans. Commun.*, vol. 47, no. 2, pp. 199–207, Feb. 1999.

[17] A. Naguib, V. Tarokh, N. Seshadri, and A. Calderbank, "A space–time coding modem for high-data-rate wireless communications," *IEEE J. Select. Areas Commun.*, vol. 16, no. 8, pp. 1459–1477, Oct. 1998.

[18] L. Aydin, E. Esteves, and R. Padovani, "Reverse link capacity and coverage improvement for CDMA cellular systems using polarization and spatial diversity," in *Proc. IEEE Int. Conf. Communications*, New York, Apr./May 2002, vol. 3, pp. 1887–1892, IEEE.

[19] G. Tavik, C. Hilterbrick, J. Evins, J. Alter, J. Crnkovich, J. G., J. de Graaf, I. Habicht, W. G. Hrin, S. Lessin, D. Wu, and S. Hagewood, "The advanced multifunction RF concept," *IEEE Trans. Microwave Theory Tech.*, vol. 53, no. 3, pp. 1009–1020, Mar. 2005.

[20] H. van Trees, *Detection, Estimation and Modulation Theory, Part III*. New York: Wiley, 1971.

[21] M. Skolnik, Ed., *Radar Handbook*, 2nd ed. New York: McGraw-Hill, 1990, ISBN: 0-07-057913-X.

[22] M. J. E. Golay, "Complementary series," *IRE Trans. Inf. Theory*, vol. IT-7, no. 2, pp. 82–87, Apr. 1961.

[23] R. J. Turyn, "Ambiguity functions of complementary sequences," *IEEE Trans. Inf. Theory*, vol. IT-9, no. 1, pp. 46–47, Jan. 1963.

[24] J. S. Byrnes, "Quadrature mirror filters, low crest factor arrays, functions achieving optimal uncertainty principle bounds, and complete orthonormal sequences—A unified approach," *Appl. Comput. Harmonic Anal.*, vol. 1, pp. 261–6, 1994.

[25] N. Levanon and E. Mozeson, *Radar Signals*. New York: Wiley, 2004.
[26] W. Moran, "The mathematics of radar," in *Twentieth Century Harmonic Analysis*, J. Byrnes, Ed. Norwell, MA: Kluwer, Sep. 2001.
[27] S. U. Pillai, B. Himed, and K. Y. Li, "Orthogonal pulsing schemes for improved target detection in space based radar," in *Proc. IEEE Aerospace Conf.*, Big Sky, MT, Mar. 2005, pp. 2180–2189.
[28] D. Giuli, L. Facheris, M. Fossi, and A. Rossettini, "Simultaneous scattering matrix measurement through signal coding," in *Rec. IEEE Int. Radar Conf,*, Arlington, VA, May 1990, pp. 258–262.
[29] V. Tarokh, H. Jafarkhani, and A. Calderbank, "Space–time block codes from orthogonal designs," *IEEE Trans. Inf. Theory*, vol. 45, no. 5, pp. 1456–1467, Jul. 1999.
[30] H. Schmitt, *DARPA ISP Review, Raytheon Program*, May 2006, Wigwam Resort.
[31] S. Suvorova, B. Moran, and M. Viola, "Adaptive modeling of sea clutter and detection of small targets in heavy clutter," in *Proc. IEEE Int. Radar Conf.*, Adelaide, Australia, Sep. 2003, pp. 614–618.